UC San Diego
UC San Diego Previously Published Works

Title
Lipid raft microdomain compartmentalization of TC10 is required for insulin signaling and GLUT4 translocation

Permalink
https://escholarship.org/uc/item/6xs9j18m

Journal
Journal of Cell Biology, 154(4)

ISSN
0021-9525

Authors
Watson, Robert T
Shigematsu, Satoshi
Chiang, Shian-Huey
et al.

Publication Date
2001-08-20

DOI
10.1083/jcb.200102078

Peer reviewed

Lipid raft microdomain compartmentalization of TC10 is required for insulin signaling and GLUT4 translocation

Robert T. Watson,[1] Satoshi Shigematsu,[1] Shian-Huey Chiang,[2,3] Silvia Mora,[1] Makoto Kanzaki,[1] Ian G. Macara,[4] Alan R. Saltiel,[3] and Jeffrey E. Pessin[1]

[1]Department of Physiology and Biophysics, University of Iowa, Iowa City, IA 52242
[2]Cellular and Molecular Biology Graduate Program, University of Michigan, Ann Arbor, MI 48109
[3]Departments of Internal Medicine and Physiology, Life Sciences Institute, University of Michigan Medical Center, Ann Arbor, MI 48109
[4]Center for Cell Signaling, University of Virginia, Charlottesville, VA 22908

Recent studies indicate that insulin stimulation of glucose transporter (GLUT)4 translocation requires at least two distinct insulin receptor–mediated signals: one leading to the activation of phosphatidylinositol 3 (PI-3) kinase and the other to the activation of the small GTP binding protein TC10. We now demonstrate that TC10 is processed through the secretory membrane trafficking system and localizes to caveolin-enriched lipid raft microdomains. Although insulin activated the wild-type TC10 protein and a TC10/H-Ras chimera that were targeted to lipid raft microdomains, it was unable to activate a TC10/K-Ras chimera that was directed to the non-

lipid raft domains. Similarly, only the lipid raft–localized TC10/H-Ras chimera inhibited GLUT4 translocation, whereas the TC10/K-Ras chimera showed no significant inhibitory activity. Furthermore, disruption of lipid raft microdomains by expression of a dominant-interfering caveolin 3 mutant (Cav3/DGV) inhibited the insulin stimulation of GLUT4 translocation and TC10 lipid raft localization and activation without affecting PI-3 kinase signaling. These data demonstrate that the insulin stimulation of GLUT4 translocation in adipocytes requires the spatial separation and distinct compartmentalization of the PI-3 kinase and TC10 signaling pathways.

Introduction

The plasma membrane of most cell types contains specialized subdomains with distinct lipid and protein compositions, referred to as lipid raft microdomains (Brown and London, 1998; Kurzchalia and Parton, 1999). The selective inclusion or exclusion of key signaling molecules within lipid rafts may be one means of organizing the multitude of signals impinging on the cell surface into distinct signaling cascades (Anderson, 1998; Okamoto et al., 1998). Indeed, many members of the growth factor receptor superfamily share common intracellular signaling pathways, yet produce distinct biological responses. Spatial compartmentalization at the plasma membrane has been suggested as a possible means for preserving signaling specificity and fidelity in these cases (Smart et al., 1999; Sternberg and Schmid, 1999). One such growth factor receptor is the insulin recep-

tor, which has been reported to phosphorylate and partially colocalize with caveolin (Mastick et al., 1995; Mastick and Saltiel, 1997; Yamamoto et al., 1998; Gustavsson et al., 1999; Nystrom et al., 1999), the major structural component of a subset of lipid raft microdomains that forms characteristic invaginations of the plasma membrane termed caveolae (Brown and London, 1998; Fujimoto et al., 1998).

Of the many functions of insulin, one of the most important is to increase glucose uptake in striated muscle and adipose tissues (Czech, 1995; Summers et al., 1999). In the basal state, the insulin-responsive glucose transporter (GLUT)4* cycles slowly between the plasma membrane and one or more intracellular compartments, with the vast majority of the transporter residing within the cell interior (Martin et al., 1996a; Millar et al., 1999; Simpson et al., 2001). Insulin triggers a large increase in the rate of GLUT4 vesicle exocy-

*Abbreviations used in this paper: BFA, brefeldin A; CAP, Cbl-associated protein; GLUT, glucose transporter; HA, hemagglutinin; PI-3, phosphatidylinositol 3; TfR, transferrin receptor.

tosis, resulting in the accumulation of the transporter on the cell surface and a concomitant increase in glucose uptake (Rea and James, 1997; Pessin et al., 1999).

It has been well established that phosphatidylinositol 3 (PI-3) kinase activity is necessary for insulin-stimulated GLUT4 translocation (Cheatham et al., 1994; Okada et al., 1994; Martin et al., 1996b; Sharma et al., 1998; Czech, 2000). However, a clear demonstration for a sufficient role for PI-3 kinase has not been forthcoming. Moreover, several lines of evidence suggest that one or more PI-3 kinase–independent signals may be required for insulin-stimulated GLUT4 translocation. For example, two naturally occurring insulin receptor mutations were unable to induce GLUT4 translocation and glucose uptake, yet were fully capable of activating PI-3 kinase (Krook et al., 1997). Activation of PI-3 kinase activity through the interleukin 4 receptor or engagement of integrin receptors also failed to enhance glucose uptake and GLUT4 translocation (Isakoff et al., 1995; Guilherme and Czech, 1998). Furthermore, a cell-permeable PI(3,4,5)P3 analogue had no effect on glucose uptake (Jiang et al., 1998). Together, these data suggest that additional insulin signaling pathways may exist that function independently of the pathway defined by the PI-3 kinase.

The Cbl protooncogene is specifically tyrosine phosphorylated by the insulin receptor in adipocytes through the adapter proteins Cbl-associated protein (CAP) and APS (Ribon et al., 1998; Ahmed et al., 2000). CAP directly interacts with Cbl and appears to be important in insulin signaling, since expression of a dominant-interfering CAP mutant (CAPΔSH3) markedly inhibited insulin-stimulated glucose uptake and GLUT4 translocation (Baumann et al., 2000). More recently, we have observed that the CAP/Cbl pathway is necessary for the activation of TC10, a Rho family GTP-ase that is highly expressed in muscle and adipose tissues (Neudauer et al., 1998; Imagawa et al., 1999; Chiang et al., 2001). Here we demonstrate that TC10 localizes to caveolin-enriched lipid microdomains at the plasma membrane. Furthermore, the compartmentalization of TC10 within lipid microdomains is essential for insulin-dependent activation of TC10 and GLUT4 translocation. These data provide a molecular basis for the specificity of insulin signaling with respect to glucose transport.

Results

TC10 traffics through secretory membrane compartments en route to the plasma membrane

To examine the mechanism by which TC10 modulates insulin signaling and GLUT4 translocation, we first colabeled expressed hemagglutinin (HA)-tagged TC10 with various intracellular markers in 3T3L1 adipocytes (Fig. 1). In addition, we capitalized on the differential effects of brefeldin A (BFA) and nocodazole on endomembrane compartments to further define the TC10 localization pattern. BFA causes the Golgi stacks to collapse into the endoplasmic reticulum and the TGN to coalesce with endosomal membranes in the microtubule-organizing center (Banting and Ponnambalam, 1997; Chardin and McCormick, 1999). In contrast, the microtubule inhibitor nocodazole disrupts the Golgi apparatus into ministacks and blocks retrograde traffic between the

Golgi membranes and the endoplasmic reticulum, without inhibiting anterograde traffic to the plasma membrane (Lippincott-Schwartz et al., 1990; Kok et al., 1992).

In control cells, the cis-Golgi marker p115 showed the characteristic perinuclear distribution (Fig. 1 A, a). The expressed TC10 protein was localized to the plasma membrane and the perinuclear region that partially overlapped with p115 (Fig. 1 A, b and c). BFA treatment resulted in a dispersed labeling pattern for p115 (Fig. 1 A, d). However, TC10 displayed a persistent, concentrated labeling pattern in the presence of BFA that no longer colocalized with p115 (Fig. 1 A, e and f). Similarly, disruption of the Golgi stacks with nocodazole resulted in a dispersed labeling pattern for p115 and the default accumulation of TC10 at the plasma membrane (Fig. 1 A, g and h). Under these conditions, there was also no colocalization of TC10 with p115, indicating that the majority of the perinuclear TC10 was not localized in the cis-Golgi (Fig. 1 A, g–i).

Syntaxin 6 is a resident protein of the TGN (Bock et al., 1996; Watson and Pessin, 2000). In contrast to the results obtained above with p115, TC10 showed substantial perinuclear overlap with syntaxin 6 in both control cells and in cells treated with BFA (Fig. 1 B, a–f). Nocodazole treatment resulted in a punctate distribution of syntaxin 6 and the accumulation of TC10 at the cell surface (Fig. 1 B, g–i). The transferrin receptor (TfR) cycles between the cell surface and endosome compartments, where it often shows strong perinuclear labeling (Fig. 1 C, a). In control and BFA-treated cells, TfR also displayed a strong overlap with TC10 (Fig. 1 C, a–f). As described above, in the presence of nocodazole TC10 was found predominantly at the plasma membrane, where it overlapped with TfR (Fig. 1 C, g–i). Together, these results indicate that TC10 is largely present in the plasma membrane and the perinuclear-recycling endosome compartment, although we can not unambiguously distinguish between recycling endosomes and the TGN in adipocytes.

Since TC10 is predicted to be both farnesylated and palmitoylated at the COOH-terminus (Fig. 2 A), TC10 most likely transits through the secretory membrane system en route to the plasma membrane, in an identical manner to that established for H-Ras and several other proteins that undergo posttranslational prenylation and palmitoylation (Choy et al., 1999; Resh, 1999; Apolloni et al., 2000; Michaelson et al., 2001). Indeed, the TC10 expression pattern was essentially indistinguishable from the subcellular distribution of H-Ras, both in control cells and cells treated with BFA or nocodazole (Fig. 1 D, a–i). Furthermore, incubation of cells with cycloheximide subsequent to transfection resulted in the rapid and identical chase (<4 h) of the entire endomembrane pool of both H-Ras and TC10 to the plasma membrane (data not shown). Thus, TC10 appears to be processed through the secretory membrane system and perinuclear–recycling endosomes during its transit to the plasma membrane in a manner similar to that described recently for H-Ras (Prior and Hancock, 2001).

TC10 is functionally restricted by COOH-terminal targeting sequences

Recent studies have documented that the COOH-terminal domains of the small GTP binding proteins of the Ras and
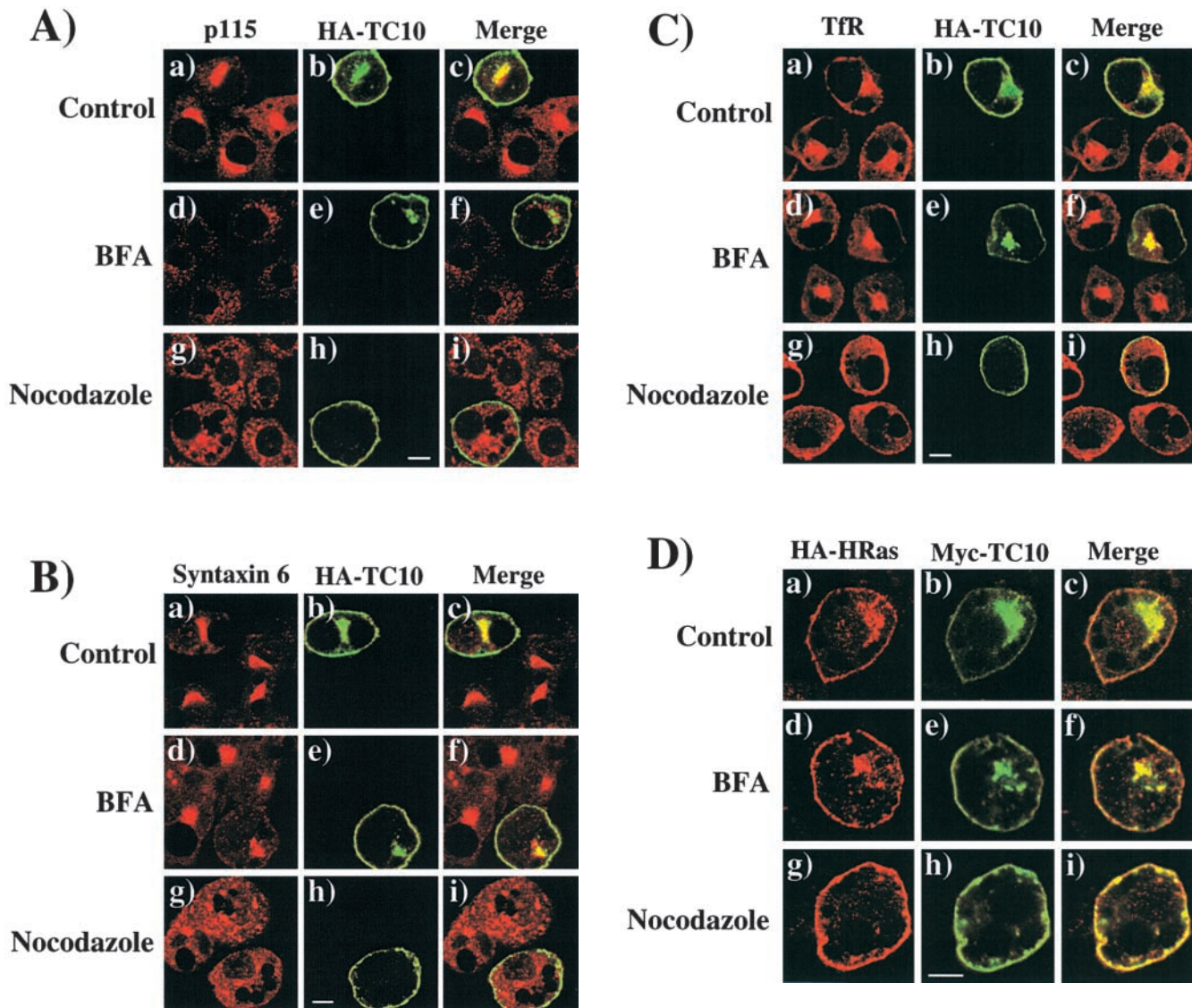
Figure 1. **Expressed TC10 localizes to the plasma membrane and a subset of endomembrane compartments in 3T3L1 adipocytes.** (A) Differentiated 3T3L1 adipocytes were electroporated with 50 µg of the cDNA encoding for the full length TC10 protein containing an NH_2-terminal HA-epitope tag as described in Materials and methods. 18 h later, the cells were either left untreated (a–c) or incubated with 10 µM BFA (d–f) for 60 min or 33 µM nocodazole (g–i) for 3 h at 37°C. The cells were then fixed and colabeled with a polyclonal HA antibody (b, e, and h) and either (A) monoclonal antibody for p115 (a, d, and g), (B) monoclonal antibody for syntaxin 6 (a, d, and g), or (C) monoclonal antibody for TfR (a, d, and g). (D) The cells were cotransfected with HA-HRas (50 µg) and Myc-TC10 (50 µg) and treated as described above. The cells were then labeled with a polyclonal HA antibody (a, d, and g) and a monoclonal Myc antibody (b, e, and h). The merged images for each individual condition are presented in c, f, and i. These are representative cells from three independent determinations. Bar, 10 µM.

Rho families direct different intracellular trafficking routes and plasma membrane subdomain compartmentalization (Choy et al., 1999; Roy et al., 1999; Apolloni et al., 2000; Michaelson et al., 2001). In contrast to the trafficking and localization of H-Ras to caveolin-enriched plasma membrane microdomains, K-Ras is excluded from the secretory membrane system and inserts into nonlipid raft domains of the plasma membrane. Moreover, even though H-Ras and K-Ras contain identical effector domains, this microdomain localization appears to account for the different signaling properties of H-Ras compared with K-Ras (Roy et al., 1999; Walsh and Bar-Sagi, 2001). Inspection of the COOH-terminal sequences indicates that TC10 should undergo posttranslational modifications similar to H-Ras, which has cysteine

residues in the appropriate contexts for both farnesylation and palmitoylation (Fig. 2 A). Therefore, to examine the role of the COOH-terminus in the localization of TC10, we generated chimeric TC10 proteins containing the COOH-terminal domains of H-Ras (TC10/H-Ras) and K-Ras (TC10/K-Ras). As typically observed, wild-type TC10 displayed both perinuclear and plasma membrane localization identical to H-Ras (Fig. 2 B, a and b). In contrast, K-Ras exclusively localized to the plasma membrane with very low levels detectable in any intracellular compartment (Fig. 2 B, c). As expected, the TC10/H-Ras chimera was distributed in a manner indistinguishable from both wild-type TC10 and H-Ras, whereas the TC10/K-Ras chimera was distributed in a manner indistinguishable from K-Ras (Fig. 2 B, d and e).

Figure 2. **The endomembrane trafficking and plasma membrane subdomain compartmentalization of TC10 is defined by the COOH-terminal domain.** (A) Amino acid sequence comparison of the COOH-terminal 22 amino acids of TC10, H-Ras, K-Ras, TC10/H-Ras chimera, and TC10/K-Ras chimera. (B) Differentiated 3T3L1 adipocytes were electroporated with 50 μg of the HA epitope–tagged TC10 (a), H-Ras (b), K-Ras (c), TC10/H-Ras chimera (d), and TC10/K-Ras chimera (e) cDNAs as described in Materials and methods. 18 h later, the cells were fixed and the subcellular localization was determined by confocal fluorescent microscopy. (C) Differentiated 3T3L1 adipocytes were coelectroporated with 50 μg of GLUT4-EGFP plus 200 μg of the empty vector (a and b), TC10 (c and d), H-Ras (e and f), K-Ras (g and h), TC10/H-Ras chimera (i and j), and TC10/K-Ras chimera (k and l) cDNAs. 18 h later, the cells were then incubated for 30 min in the absence (a, c, e, g, i, and k) or presence (b, d, f, h, j, and l) of 100 nM insulin. The cells were then fixed and the subcellular localization was determined by confocal fluorescent microscopy. These are a representative field of cells from five or six independent determinations. (D) Quantitation of the number of cells displaying GLUT4-EGFP plasma membrane fluorescent was determined from the counting of 175–200 cells that were coexpressing both the TC10 constructs and GLUT4-EGFP in five or six independent experiments. Bar, 10 μM.
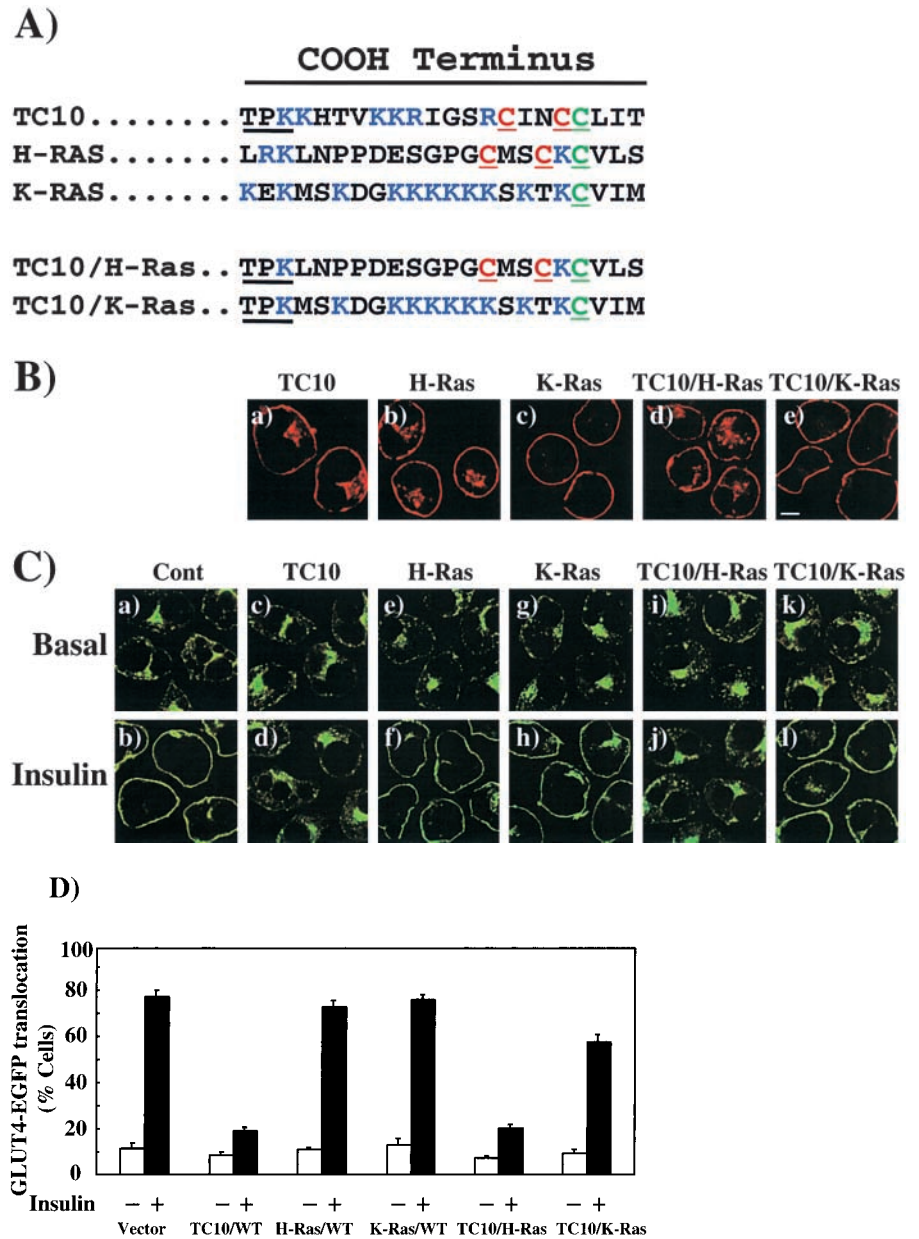
To determine whether the inhibitory property of TC10 was dependent on subdomain compartmentalization, we next cotransfected the TC10/H-Ras or TC10/K-Ras chimeras with GLUT4-EGFP. Insulin stimulation resulted in the appearance of a strong plasma membrane GLUT4-EGFP rim fluorescence, indicative of translocation (Fig. 2 C, a and b). Similar to our previous findings, coexpression of wild-type TC10 strongly inhibited GLUT4 translocation, whereas H-Ras and K-Ras were without any significant effect (Fig. 2 C, c–h). Although the TC10/H-Ras chimera potently inhibited GLUT4-EGFP translocation in a manner identical to wild-type TC10, the TC10/K-Ras chimera behaved like K-Ras and had no effect on GLUT4-EGFP translocation (Fig. 2 C, i–l). These data were quantitated by determining the number of cells displaying a continuous cell surface GLUT4-EGFP fluorescence (Fig. 2 D).

We next determined whether TC10 subdomain compartmentalization was important for its activation by insulin (Fig. 3). Using a GST-Pak1 pull down assay to precipitate the GTP-bound TC10 protein, we observed that insulin produced a time-dependent activation of the expressed wild-type TC10 protein (Fig. 3 A, lanes 1–5). Similarly, insulin activated the TC10/H-Ras chimera over the same time frame (Fig. 3 B, lanes 1–5). However, insulin was unable to activate the TC10/K-Ras chimera under the identical conditions (Fig. 3 C, lanes 1–5). In parallel, immunoblots of cell lysates demonstrated equal amounts of TC10 expression under all these conditions. Quantitation of these data demonstrated that insulin activated TC10/WT and TC10/H-Ras 1.7 ± 0.4- and 1.7 ± 0.3-fold, respectively. In contrast, TC10/K-Ras was not significantly activated by insulin (0.9 ± 0.1). Thus, these data demonstrate that the upstream pathway required for insulin-dependent activation of TC10 is also con-
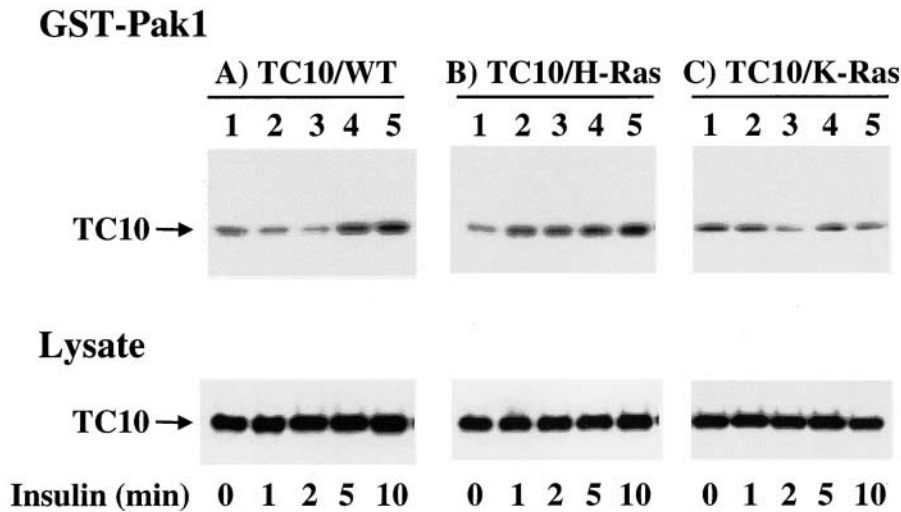
GST-Pak1

Figure 3. **Insulin activates TC10 only when specifically targeted by the TC10 and H-Ras COOH-terminal domains.** Differentiated 3T3L1 adipocytes were electroporated with (A) 50 μg of HA-TC10/WT, (B) HA-TC10/H-Ras chimera, and (C) HA-TC10/K-Ras chimera cDNAs as described in Materials and methods. 48 h later, the cells were incubated in the absence (lane 1) or the presence of 100 nM insulin for 1 (lane 2), 2 (lane 3), 5 (lane 4), and 10 (lane 5) min. Cell lysates were then prepared and either directly immunoblotted for TC10 expression (Lysate) or precipitated with 6 μg of the GST-Pak1 Crib domain fusion. The precipitates were then solubilized and immunoblotted for TC10 (GST-Pak1). This is a representative immunoblot from two to four independent determinations.

fined to the same specific lipid raft microdomain defined by the COOH-terminal H-Ras and TC10 targeting sequences.

TC10 is localized to caveolae-enriched plasma membrane microdomains

To determine whether the endogenous TC10 protein was localized to plasma membrane lipid raft microdomains, adipocytes were first colabeled with monoclonal caveolin and polyclonal TC10 antibodies. In intact cells, the endogenous TC10 protein was predominantly confined to the plasma membrane with very little detectable expression on intracellular membranes (Fig. 4, a and c). Similarly, caveolin displayed strong plasma membrane localization with lower, but still detectable, levels in the perinuclear region (Fig. 4, b and c). We also prepared plasma membrane sheets and examined the localization patterns of TC10 and caveolin. Although individual caveolae (50–80 nm) are too small to be detected by laser confocal microscopy, caveolae can form large clusters or torus-shaped structures in adipocytes (Gustavsson et al., 1999). Endogenous TC10 was found to colocalize exceptionally well with caveolin in these distinct ring-like domains at the plasma membrane (Fig. 4, d–f).

The organization of the large, caveolin-positive structures was examined at higher magnification (Fig. 5 A, a and b). These torus-shaped configurations were found to range in size from 0.5 to 1.5 μm. The assembly of individual caveolae into these ringed structures was confirmed by caveolin-immunogold electron microscopy (Fig. 5 B, a and b). At low magnification, both individual and multiple aggregates of immunopositive caveolin–labeled structures were present in the adipocyte plasma membrane (Fig. 5 B, a). At higher magnification, these aggregates of caveolin-positive structures were clearly visualized as clusters of individual immunopositive caveolae organized into ring-like shapes. Furthermore, the size distribution of these aggregates were in excellent agreement with the dimensions determined by confocal fluorescent microscopy.

The morphological effects of cholesterol extraction on these caveolin-positive structures were examined in Fig. 6. Previous studies have demonstrated that treatment of cells
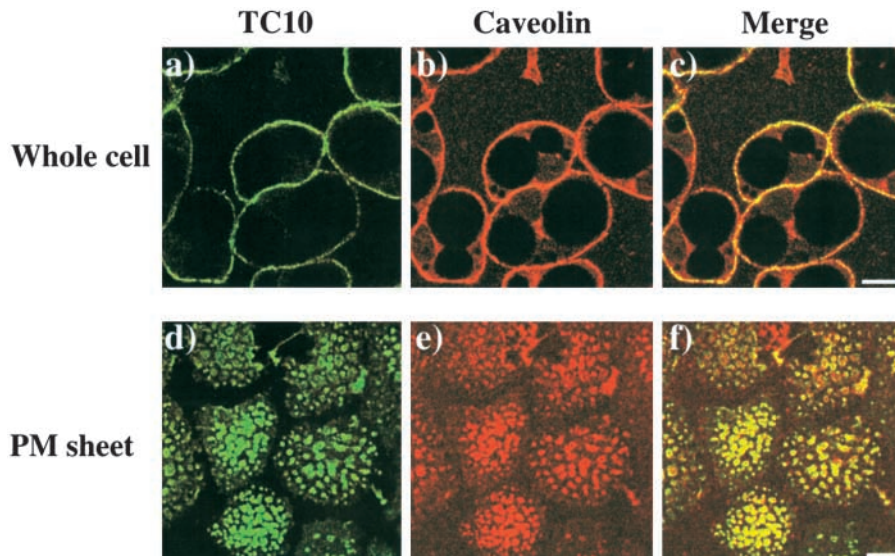

Figure 4. **Endogenous TC10 colocalizes with caveolin-positive structures in the adipocyte plasma membrane.** Differentiated 3T3L1 adipocytes were left untreated and either the intact cells were directly fixed (a–c), or used to isolated plasma membrane sheets (d–f) as described in Materials and methods. The samples were then colabeled with a polyclonal TC10 antibody (a and b) and a monoclonal caveolin 1 antibody (b and e) and subjected confocal fluorescent microscopy. The merged images are presented in panels c and f. These are representative fields from three independent determinations. Bar, 10 μM.

Figure 5. **Individual plasma membrane caveolae are clustered into higher-order structures in adipocytes**. (A) Plasma membrane sheets were prepared from differentiated 3T3L1 adipocytes, incubated with a monoclonal caveolin 1 antibody, and subjected to confocal fluorescent microscopy at low magnification (a) or at high magnification (b) as indicated by the inset bar. (B) Plasma membrane sheets were prepared, fixed, and incubated with a monoclonal caveolin 1 antibody and a 10-nm gold-conjugated rabbit anti–mouse antibody as described in Materials and methods. The samples where then sectioned and visualized at low magnification (a) or high magnification (b) as indicated by the inset bar. Arrowheads indicate caveolae clustered into ring-shaped structures and arrows indicate individual caveolae.
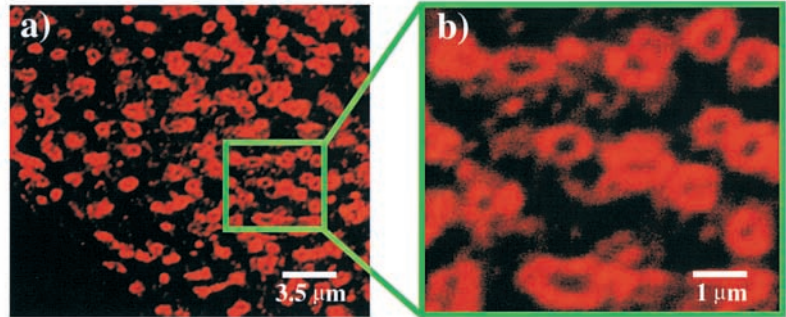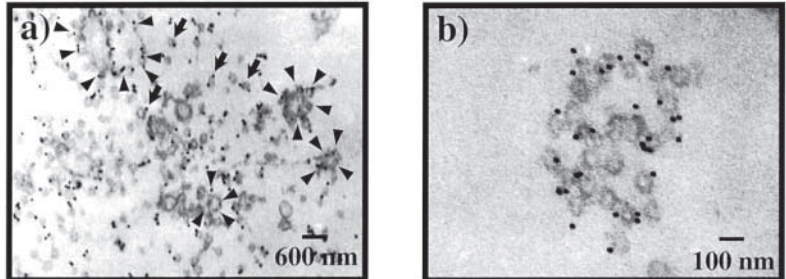
with methyl-β-cyclodextrin (β-CD) results in cholesterol depletion and disruption of plasma membrane caveolae (Chang et al., 1992; Rothberg et al., 1992; Hailstones et al., 1998; Parpal et al., 2001). Similarly, treatment of adipocytes with β-CD resulted in a time-dependent dissolution of these torus-shaped caveolin structures, which was nearly complete by 60 min (Fig. 6, a–e). In addition, treatment with β-CD resulted in a parallel disruption of TC10 organization and colocalization with caveolin (Fig. 6, f–o). Thus, these data

demonstrate that the adipocyte plasma membrane has highly organized aggregates of individual caveolin-enriched lipid rafts that form large morphologically distinct torus-shaped structures.

To confirm the plasma membrane compartmentalization of the expressed TC10 and TC10/Ras chimera proteins, we next compared their colocalization with caveolin in isolated plasma membrane sheets. As reported previously (Li et al., 1996; Mineo et al., 1996; Song et al., 1996; Roy et al., 1999), H-Ras was found to colocalize with the caveolin-pos-
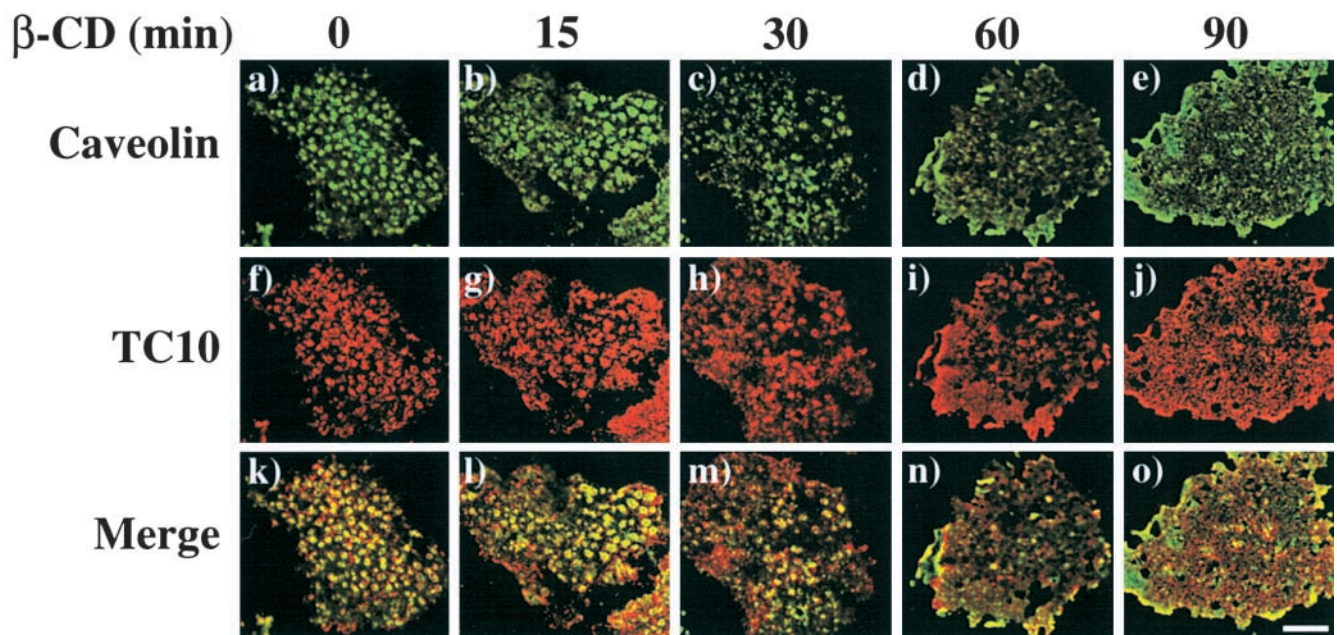

Figure 6. **Cholesterol depletion with methyl-β-cyclodextrin disrupts the plasma membrane subdomain compartmentalization of caveolin and TC10.** Differentiated 3T3L1 adipocytes were incubated with 10 mM β-CD for the times indicated. Plasma membrane sheets were prepared and colabeled with a rabbit caveolin 1 antibody (a–e) and a chicken TC10 antibody (f–j). Merged images are presented in panels k–o. These are representative plasma membrane sheets from two independent determinations. Bar, 10 μM.
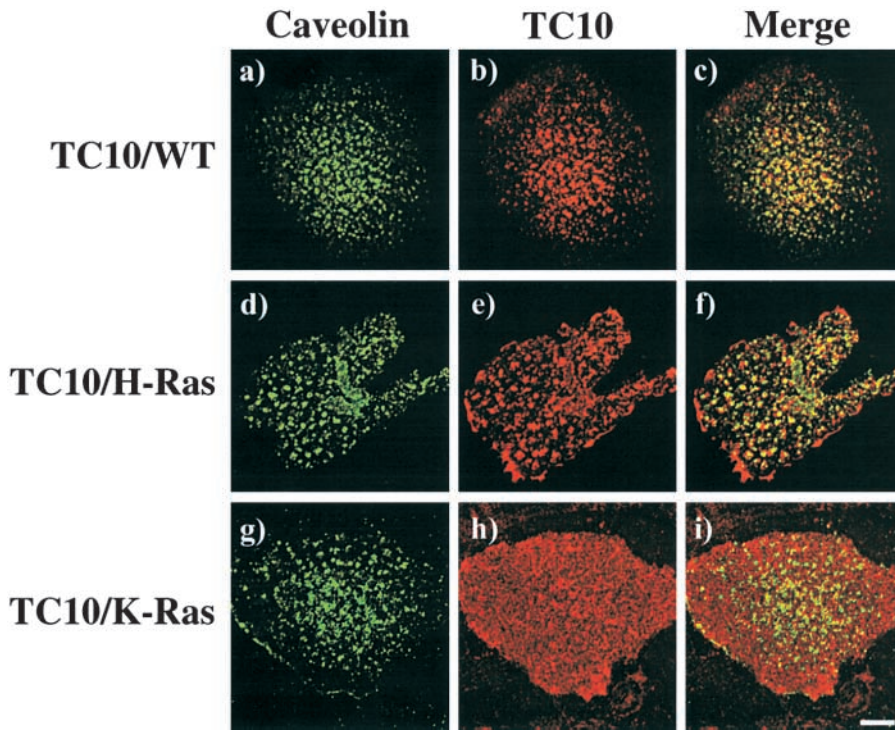
Figure 7. **The expressed TC10/WT and TC10/H-Ras chimeras specifically colocalize with caveolin.** Differentiated 3T3L1 adipocytes were electroporated with 50 μg of HA epitope–tagged TC10 (a–c), TC10/H-Ras chimera (d–f), and TC10/K-Ras chimera (g–i) cDNAs, and plasma membrane sheets were prepared 18 h later. The plasma membrane sheets were then colabeled with a polyclonal caveolin 1 antibody (a, d, and g) and a monoclonal HA antibody (b, e, and h). Merged images are presented in panels c, f, and i. These are representative plasma membrane sheets from three independent determinations.

itive torus-shaped structures, whereas K-Ras was uniformly distributed across the plasma membrane sheets and did not specifically colocalize with caveolin (data not shown). As observed for the endogenous TC10 protein, the expressed TC10/WT protein was strongly colocalized with caveolin in the torus-shaped structures (Fig. 7, a–c). A similar plasma membrane distribution was detected for the expressed TC10/H-Ras chimera (Fig. 7, d–f). In contrast, the TC10/ K-Ras chimera was found to be uniformly scattered throughout the plasma membrane (Fig. 7, g–i).

Disruption of lipid raft microdomains with a dominant-interfering caveolin mutant (Cav3/DGV) mislocalizes TC10 and inhibits GLUT4 translocation

A dominant-interfering caveolin 3 mutant (Cav3/DGV) has been found to sequester cholesterol away from the endoge-
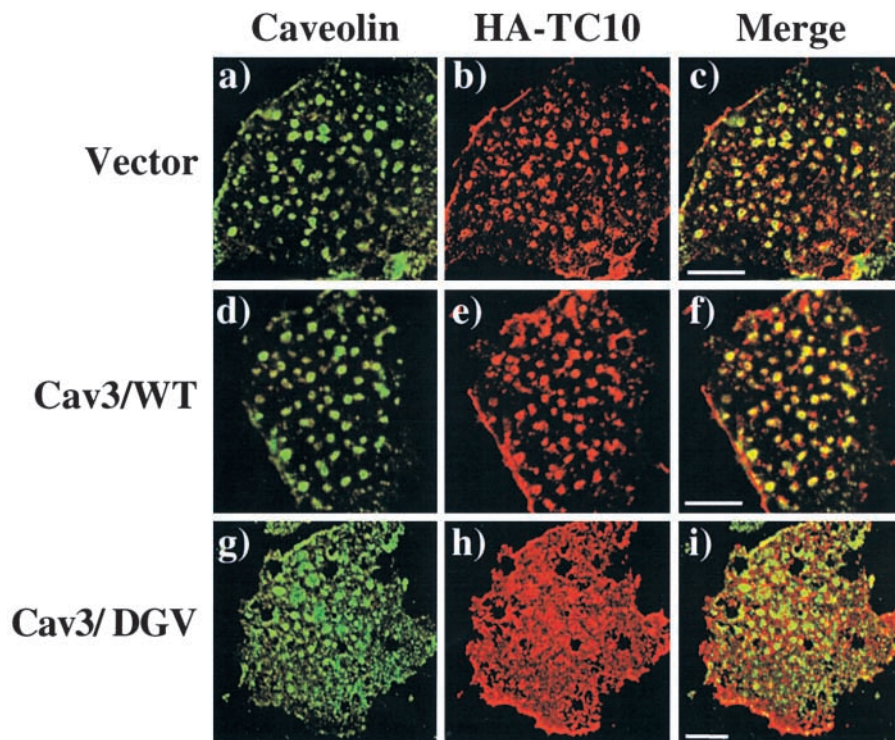

Figure 8. **Expression of a dominant-interfering caveolin 3 mutant disrupts the plasma membrane subdomain compartmentalization of TC10.** Differentiated 3T3L1 adipocytes were coelectroporated with 50 μg of HA-TC10 plus 200 μg of the empty vector (a–c), wild-type caveolin 3 (Cav3/WT; d–f), or the dominant-interfering caveolin 3 mutant (Cav3/DGV; g–i). 36 h later, the cells were fixed, plasma membrane sheets were prepared and subjected to confocal fluorescent microscopy with a polyclonal caveolin 1 antibody (a, d, and g), and a monoclonal HA antibody (b, e, and h). The merged images are shown in panels c, f, and i. These are representative field of cells from two independent determinations. Bar, 10 μM.

Figure 9. **Expression of a dominant-interfering caveolin 3 mutant inhibits insulin-stimulated GLUT4 transloca-tion**. (A) Differentiated 3T3L1 adipocytes were coelectroporated with 50 μg of GLUT4-EGFP plus 200 μg of the empty vector (a and b), Myc epitope–tagged wild-type caveolin 3 (Cav3/WT; c and d), or Myc epitope tagged domi-nant-interfering caveolin 3 mutant (Cav3/DGV; e and f). 36 h later, the cells were then incubated for 30 min in the absence (a, c, and e) or presence (b, d, and f) of 100 nM insulin. The cells were then fixed and the subcellular localization of GLUT4-EGFP was determined by confocal fluorescent microscopy. These are a representative field of cells from four independent determinations. (B) The subcellular distribution of expressed Cav3/WT (a and b) or the Cav3/DGV mutant (c and d) was determined by confocal fluorescent microscopy. These are a representative field of cells from four independent determinations. Bar, 10 μM.
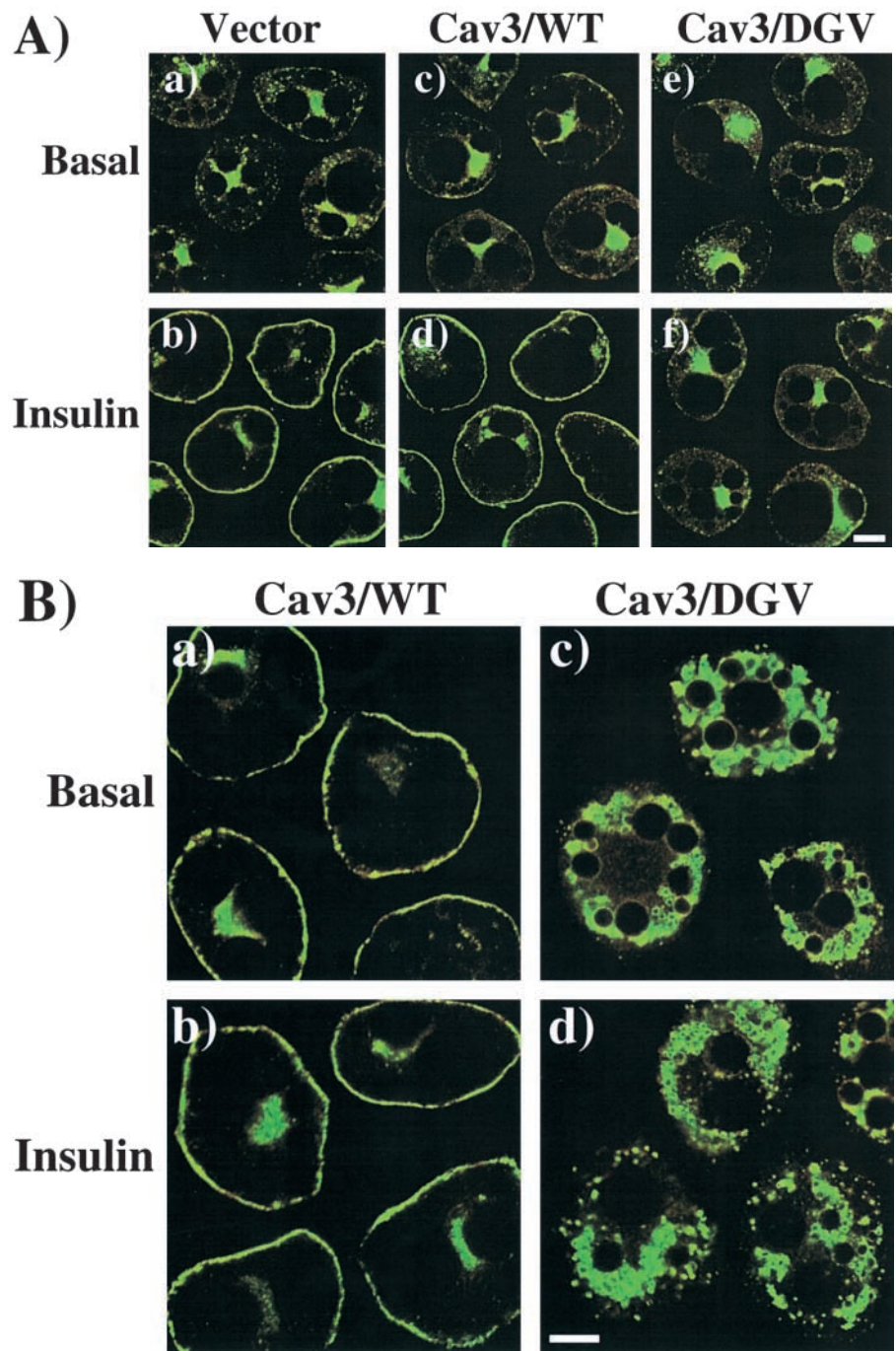
nous lipid raft microdomains (Roy et al., 1999; Pol et al., 2001). Furthermore, expression of the Cav3/DGV mutant partially misdirected H-Ras out of membrane microdomains and functionally inhibited H-Ras, but not K-Ras, signaling responses (Roy et al., 1999). Since TC10 localizes to caveo-lar structures and shows a trafficking pattern indistinguish-able from H-Ras, we determined whether the Cav3/DGV mutant would also effect the plasma membrane micro-domain distribution of TC10. Similar to the endogenous TC10 protein, the expressed EGFP-TC10/WT fusion pro-tein was colocalized with endogenous plasma membrane ca-veolin in the torus-shaped structures (Fig. 8, a–c). Similarly, expression of Cav3/WT had no significant effect on the plasma membrane microdomain localization of either the coexpressed EGFP-TC10 protein or on endogenous caveo-lin (Fig. 8, d–f). In contrast, expression of Cav3/DGV re-sulted in a partial dispersion of caveolin concomitant with a marked reduction in the number of torus-shaped caveolin-positive structures (Fig. 8 g). More importantly, there was a near complete scattering of TC10 throughout the plasma membrane (Fig. 8, h and i). The greater effect of Cav3/DGV on TC10 compared with caveolin parallels the effect of Cav3/DGV on the plasma membrane microdomain dis-tribution of caveolin and H-Ras reported previously for fi-broblasts (Roy et al., 1999). In any case, the ability of Cav3/DGV to disrupt the plasma membrane organization of
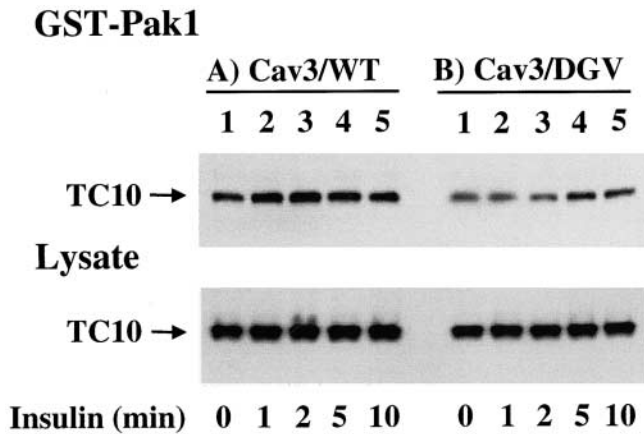
GST-Pak1

Figure 10. **Expression of a dominant-interfering caveolin 3 mutant inhibits insulin-stimulated TC10 activation.** Differentiated 3T3L1 adipocytes were electroporated with 50 μg of HA-TC10/WT cDNA plus 200 μg of Cav3/WT (A) or Cav3/DGV (B) cDNAs. 48 h later, the cells were incubated in the absence (lane 1) or the presence of 100 nM insulin for 1 (lane 2), 2 (lane 3), 5 (lane 4), and 10 (lane 5) min. Cell lysates were then prepared and either directly immunoblotted for TC10 expression (Lysate) or precipitated with 6 μg of the GST-Pak1 CRIB domain fusion. The precipitates were then solubilized and immunoblotted for TC10 (GST-Pak1). This is a representative immunoblot from three independent determinations.

TC10 is consistent with the effect of β-CD and further supports the specific plasma membrane microdomain compartmentalization of TC10.

Based on these results, we next examined the effect of Cav3/DGV on insulin-stimulated GLUT4 translocation (Fig. 9). Expression of the wild-type caveolin 3 protein (Cav3/WT) had no effect on GLUT4-EGFP translocation, which was essentially identical to the control transfected cells (Fig. 9 A, a–d). In contrast, the Cav3/DGV mutant inhibited insulin-stimulated GLUT4-EGFP translocation (Fig. 9 A, e and f). The expression patterns of the Cav3/WT and Cav3/DGV constructs were also determined (Fig. 9 B). As reported previously, Cav3/WT was predominantly localized to the plasma membrane, with a small amount also present in the perinuclear region (Fig. 9 B, a and b). In contrast, Cav3/DGV showed strong labeling in the cytoplasm, where it formed distinct vesicle structures (Fig. 9 B, c and d) similar to the cholesterol-enriched vesicles previously reported in fibroblasts (Roy et al., 1999; Pol et al., 2001). Insulin stimulation had no significant effect on the localization of either Cav3/WT or Cav3/DGV (Fig. 9 B, a–d).

Since the insulin activation of TC10 requires the appropriate COOH-terminal domain targeting sequences (Fig. 3), we next determined the effect of Cav3/DGV on insulin-stimulated TC10 activation (Fig. 10). Coexpression of HA-TC10/WT with Cav3/WT had no significant effect on the insulin stimulation of TC10 activation (Fig. 10 A, lanes 1–5). In contrast, expression of Cav3/DGV resulted in marked inhibition in the time and extent of insulin-stimulated TC10 activation (Fig. 10 B, lanes 1–5). Quantitation of these data demonstrated that the maximum insulin-stimulated activation of TC10/WT in the Cav3/WT expressing cells was 1.6 ± 0.3-fold. However, in the presence of Cav3/DGV insulin was only able to activate TC10 1.0 ± 0.1-fold. The effect of

Cav3/DGV was specific for TC10 activation, as there was no detectable effect on insulin-stimulated insulin receptor autophosphorylation, IRS tyrosine phosphorylation, PI(3,4,5)P3 production, or PKB/Akt activation (data not shown).

Discussion

Emerging evidence has begun to elucidate a novel insulin receptor–signaling cascade that functions in concert with, but independent of, the PI-3 kinase pathway mediating the translocation of intracellular GLUT4 storage compartments to the cell surface. In adipocytes, this pathway involves the insulin receptor–dependent tyrosine phosphorylation of Cbl and its recruitment to lipid raft domains through the adaptor proteins CAP, APS, and flotillin (Moodie et al., 1999; Ahmed et al., 2000; Baumann et al., 2000). In turn, the tyrosine-phosphorylated Cbl protein recruits the guanylnucleotide exchange factor (GEF) C3G through the small adaptor protein CrkII (Baumann et al., 2000; Chiang et al., 2001). Importantly, C3G can function as a GEF for the small GTP-binding protein TC10, and insulin stimulation converts TC10 from the inactive GDP-bound to the active GTP-bound state. Furthermore, overexpression of TC10 specifically inhibits insulin-stimulated GLUT4 translocation without any effect on other insulin-responsive vesicular compartments. Thus, we speculated that the apparent function of the insulin-dependent assembly and plasma membrane lipid raft microdomain targeting of the CAP–Cbl–CrkII–C3G signaling complex was to direct C3G to the appropriate location for efficient activation of TC10.

Although the Switch I and Switch II domains of TC10 have a high degree of sequence similarity with Rac, Rho, and Cdc42, in other respects TC10 is an unusual member of the Rho protein family. In particular, most Rho family members contain a single COOH cysteine residue in the appropriate sequence context for geranylgeranylation and interact with guanylnucleotide dissociation inhibitors (Nobes and Hall, 1995; Bar-Sagi and Hall, 2000). In contrast, the COOH-terminal region of TC10 contains sequences similar to that of H-Ras, encoding for both farnesylation and palmitoylation (Hancock et al., 1989; Seabra, 1998). Recent studies have established that these COOH-terminal posttranslational modifications provide key trafficking determinants that may underlie signaling specificity (Sternberg and Schmid, 1999). For example, after farnesylation, proteolytic trimming, and carboxylmethylation, the subsequent palmitoylation of H-Ras allows for its insertion and trafficking through the secretory membrane system (Choy et al., 1999; Apolloni et al., 2000). This trafficking pattern ultimately results in the specific targeting of H-Ras to the caveolin-enriched plasma membrane microdomains (Dupree et al., 1993; Li et al., 1996; Song et al., 1996). In contrast, COOH-terminal K-Ras sequence does not contain any upstream palmitoylated cysteines, but instead has a polybasic motif that prevents its interaction with the Golgi apparatus and directs its association with the noncaveolin regions of the plasma membrane (Hancock et al., 1990; Choy et al., 1999; Roy et al., 1999; Apolloni et al., 2000).

The data presented here demonstrate that TC10 traffics in a manner analogous to that of H-Ras. Like H-Ras, TC10

appears to transiently associate with the secretory membrane system while en route to the plasma membrane and cycle through the perinuclear-recycling endosome compartment. This was based on the ability of cycloheximide to efficiently chase TC10 out of the endomembrane system, the strong colocalization of TC10 with the transferrin receptor, and the complete loss of perinuclear localization in the presence of nocodazole. It should be noted that the apparent absence of TC10 in the perinuclear region after nocodazole treatment could reflect either a rapid exit out of the Golgi apparatus or the presence of an alternative trafficking pathway to the plasma membrane, as has been reported for Ras2 in yeast (Bartels et al., 1999). Nevertheless, in adipocytes, TC10 and H-Ras displayed indistinguishable intracellular distributions and trafficking patterns that are similar to that recently reported for TC10 in fibroblasts (Michaelson et al., 2001).

At present, the downstream effector proteins that link activated TC10 with GLUT4 translocation remain undefined. Nevertheless, the data presented here clearly demonstrate that the specific COOH-terminal targeting sequences of TC10 are essential for the insulin-dependent activation of TC10 and regulation of GLUT4 translocation. Indeed, chimeric proteins in which the 19 COOH-terminal residues of TC10 were replaced with the corresponding amino acids from H-Ras (TC10/H-Ras) resulted in functional targeting in terms of insulin-stimulated TC10 activation and inhibition of GLUT4 translocation. In contrast, the corresponding TC10/K-Ras chimera was completely refractory to insulin stimulation and had no significant inhibitory effect on GLUT4 translocation. Although we cannot completely rule out the possibility that TC10 may function within endomembrane structures, the ability of the TC10/H-Ras chimera to recapitulate wild-type TC10 function is more consistent with a model wherein TC10 operates within lipid microdomain compartments at the plasma membrane. This conclusion is further supported by the strong colocalization of TC10 and the TC10/H-Ras chimera with plasma membrane caveolae and the fact that the TC10/K-Ras chimera was specifically excluded from this plasma membrane subdomain compartment. In addition, we have demonstrated previously that the insulin-stimulated assembly of the signaling complex that activates TC10 is also localized to plasma membrane lipid raft microdomains (Chiang et al., 2001).

One interesting morphological feature of the adipocyte plasma membrane is the presence of both multiple individual caveolae and clusters of caveolae organized into large ring-shaped structures that are visualized at both the electron microscopic and light microscopy levels (Chlapowski et al., 1983; Severs, 1988; Voldstedlund et al., 1993; Gustavsson et al., 1999). Previous studies have observed that insulin-stimulated glucose uptake is inhibited by β-CD (Gustavsson et al., 1999; Parpal et al., 2001) and our data demonstrate clearly that these higher-order caveolin and TC10 aggregates are sensitive to cholesterol extraction. Consistent with a necessary role for lipid raft microdomains, expression of the dominant-interfering caveolin 3 mutant (Cav3/DGV) inhibited insulin-stimulated GLUT4 translocation and activation of TC10. Thus, these data demonstrate that lipid raft compartmentalization is necessary for TC10 function with respect to insulin-stimulated GLUT4

translocation. Importantly, these data also demonstrate that the compartmentalized insulin signals leading to TC10 activation are independent from those regulating activation of the PI-3 kinase pathway.

One issue inherent to our understanding of intracellular signaling is the mechanism by which distinct cellular responses can result from the engagement and activation of similar arrays of downstream effector proteins. Numerous models have been proposed to account for this phenomenon, including the strength of signal generation, combinatorial diversity of different effector subsets, and/or differences in the temporal and spatial activation of downstream targets. In the case of insulin action, this problem has been complicated by numerous studies demonstrating a variety of signals capable of activating the PI-3 kinase pathway, yet unable to stimulate GLUT4 translocation or glucose transport (Weise et al., 1995; Krook et al., 1997; Guilherme and Czech, 1998; Jiang et al., 1998). In contrast, the activation of TC10 by insulin in adipocytes is not reproduced by other growth factors and requires the assembly of established signaling components in a spatially restricted subcompartment of the plasma membrane. Thus, insulin receptor signaling specificity, at least for GLUT4 translocation, appears to result from a combination of both general activation of a PI-3 kinase signal in conjunction with a spatially restricted and cell type-specific effector activation.

Materials and methods

Antibodies
The syntaxin 6, caveolin 1, caveolin 2, and p115 antibodies were purchased from Transduction Laboratories. The transferrin receptor, phospho-PKB (Ser473), and HA epitope tag antibodies were obtained from Leinco Technologies, Cell Signaling Technology, and Covance Research Products, respectively. A rabbit TC10 polyclonal antibody was prepared against the PASYHNVQEEWVPELKDCMP peptide sequence, which also cross-reacts with TCL (TC10-Like), a newly characterized isoform (Vignal et al., 2000). We also generated a chicken TC10 polyclonal antibody directed against the CZKEEWVPELKEYAP peptide sequence. Antibodies were affinity-purified using the amino-link plus immobilization kit (Pierce Chemical Co.).

Cell culture and transient transfection of 3T3L1 adipocytes
Murine 3T3L1 preadipocytes were purchased from the American Type Tissue Culture Collection. Cells were cultured in DME supplemented with 25 mM glucose and 10% calf serum at 37°C with 8% CO_2. Cells were differentiated and transfected by electroporation as described previously (Watson and Pessin, 2000). The cells were then plated on glass coverslips and stimulated with 100 nM insulin for 30 min.

Immunofluorescence and image analysis
Transfected adipocytes were washed in PBS and fixed for 15 min in 4% paraformaldehyde containing 0.2% Triton X-100, washed in PBS, and blocked in 5% donkey serum plus 1% BSA (both from Sigma-Aldrich) for 1 h. Primary and secondary antibodies were used at 1:100 dilutions (unless otherwise indicated) in blocking solution and samples were mounted on glass slides with Vectashield (Vector Laboratories). Cells were imaged using confocal fluorescence microscopy. Images were then imported into Adobe Photoshop® (Adobe Systems, Inc.) for processing and composite files were generated.

Preparation and processing of plasma membrane sheets
Adipocyte plasma membrane sheets were prepared as described previously (Robinson et al., 1992). The membrane sheets were fixed in 2% paraformaldehyde at room temperature for 20 min and blocked with 5% donkey serum. Membrane sheets were incubated with rabbit polyclonal TC10 antibody (10 µg/ml) and caveolin 2 monoclonal antibody (1:10) for 90 min at 37°C. Primary antibodies were detected with Texas red dye–conjugated donkey anti–mouse antibody and FITC-conjugated donkey anti–

rabbit antibody for 2 h at room temperature. To detect expressed TC10 and TC10/Ras chimeras in plasma membrane sheets, the electroporated cells were plated on collagen-coated coverslips and allowed to recover for 18 h in complete media. Cells were then osmotically swelled in hypotonic buffer and fixed in 2% paraformaldehyde/PBS for 10 min before sonication. Membrane sheets were then processed as described above and the expressed TC10 constructs were detected with an HA antibody (1:100) and a caveolin 1 antibody (1:250).

Cholesterol extraction
Methyl-β-cyclodextrin was added directly to serum-free DME at a final concentration of 10 mM and the cells were incubated at 37°C for various times. Plasma membrane sheets were prepared as described above.

Electron microscopy
Plasma membrane sheets were prepared as described above except that they were fixed with a combination of 4% paraformaldehyde and 0.05% glutaraldehyde for 30 min. The samples were then incubated with a monoclonal caveolin 1 antibody followed by a 10-nm gold-conjugated rabbit anti–mouse antibody. The sheets were then extensively washed and fixed a second time with 2.5% glutaraldehyde and 0.1 M sodium cacodylate, pH 7.2, followed by staining with 1% osmium tetraoxide, 1.5% potassium ferrocyanide, and 0.1 M sodium cacodylate, pH 7.2. The plasma membrane sheets were dehydrated by serial extracts with ethanol, embedded in eponate-12, sliced on a microtome, and visualized by transmission electron microscopy.

TC10/Ras chimeric constructs and DNA cloning
The TC10/H-Ras and TC10/K-Ras chimeras were generated using the PCR-based overlap extension method as described (Horton et al., 1993). In brief, the COOH-terminal 19 amino acids of TC10 (KHTVKKRIGSRCINC-CLIT) were replaced with either the final 19 amino acids of H-Ras (LNPP-DESGPGCMSCKCVLS) or the final 19 amino acids of K-Ras (MSKDGKKK-KKKSKTKCVIM). The mouse caveolin-3 cDNA was purchased from the American Type Culture Collection and subcloned into the pcDNA3.1/Myc-HIS vector (Invitrogen). To generate the Cav3/DGV mutant, PCR was used to remove the NH_2-terminal 54 amino acids from caveolin 3 (Roy et al., 1999).

Affinity precipitation of TC10 using GST-Pak1/CRIB domain
Precipitation of activated (GTP-bound) TC10 using the GST-Pak1/CRIB domain fusion protein was performed as described previously (Baumann et al., 2000). In brief, cell lysates in a volume of 100 μl were incubated for 1 h at 4°C with 200 μl of binding buffer (25 mM Tris, pH 7.5, 1 mM DTT, 30 mM MgCl$_2$, 40 mM NaCl, 0.5% NP-40) in the presence of 8 μg of GST-Pak1/CRIB coupled to glutathione-Sepharose 4B beads. The beads were then washed three times with 25 mM Tris, pH 7.5, 1 mM DTT, 30 mM MgCl$_2$, 40 mM NaCl, 1% NP-40 and once with the same buffer without NP-40. The beads were suspended in 20 μl Laemmli sample buffer. Proteins were separated by 4–20% SDS-PAGE, transferred to nitrocellulose membrane and blotted with a HA monoclonal antibody, and detected by chemiluminescence (New England Nuclear).

References

Ahmed, Z., B.J. Smith, and T.S. Pillay. 2000. The APS adapter protein couples the insulin receptor to the phosphorylation of c-Cbl and facilitates ligand-stimulated ubiquitination of the insulin receptor. *FEBS Lett.* 475:31–34.

Anderson, R.G. 1998. The caveolae membrane system. *Annu. Rev. Biochem.* 67:199–225.

Apolloni, A., I.A. Prior, M. Lindsay, R.G. Parton, and J.F. Hancock. 2000. H-ras but not K-ras traffics to the plasma membrane through the exocytic pathway. *Mol. Cell. Biol.* 20:2475–2487.

Banting, G., and S. Ponnambalam. 1997. TGN38 and its orthologues: roles in post-TGN vesicle formation and maintenance of TGN morphology. *Biochim. Biophys. Acta.* 1355:209–217.

Bar-Sagi, D., and A. Hall. 2000. Ras and Rho GTPases: a family reunion. *Cell.* 103:227–231.

Bartels, D.J., D.A. Mitchell, X. Dong, and R.J. Deschenes. 1999. Erf2, a novel gene product that affects the localization and palmitoylation of Ras2 in *Saccharomyces cerevisiae*. *Mol. Cell. Biol.* 19:6775–6787.

Baumann, C.A., V. Ribon, K. Kanzaki, D.C. Thurmond, S. Mora, S. Shigematsu, P.E. Bickel, J.E. Pessin, and A.R. Saltiel. 2000. CAP defines a second signaling pathway required for insulin-stimulated glucose transport. *Nature.* 407:202–207.

Bock, J.B., R.C. Lin, and R.H. Scheller. 1996. A new syntaxin family member implicated in targeting of intracellular transport vesicles. *J. Biol. Chem.* 271:17961–17965.

Brown, D.A., and E. London. 1998. Functions of lipid rafts in biological membranes. *Annu. Rev. Cell Dev. Biol.* 14:111–136.

Chang, W.J., K.G. Rothberg, B.A. Kamen, and R.G. Anderson. 1992. Lowering the cholesterol content of MA104 cells inhibits receptor-mediated transport of folate. *J. Cell Biol.* 118:63–69.

Chardin, P., and F. McCormick. 1999. Brefeldin A: the advantage of being uncompetitive. *Cell.* 97:153–155.

Cheatham, B., C.J. Vlahos, L. Cheatham, L. Wang, J. Blenis, and C.R. Kahn. 1994. Phosphatidylinositol 3-kinase activation is required for insulin stimulation of pp70 S6 kinase, DNA synthesis, and glucose transporter translocation. *Mol. Cell. Biol.* 14:4902–4911.

Chiang, S.H., C.A. Baumann, M. Kanzaki, D.C. Thurmond, R.T. Watson, C.L. Neudauer, I.G. Macara, J.E. Pessin, and A.R. Saltiel. 2001. Insulin-stimulated GLUT4 translocation requires the CAP-dependent activation of TC10. *Nature.* 410:944–948.

Chlapowski, F.J., B.K. Bertrand, J.E. Pessin, Y. Oka, and M.P. Czech. 1983. The relationship of microvesicles to the plasmalemma of rat adipocytes. *Eur. J. Cell Biol.* 32:24–30.

Choy, E., V.K. Chiu, J. Silletti, M. Feoktistov, T. Morimoto, D. Michaelson, I.E. Ivanov, and M.R. Philips. 1999. Endomembrane trafficking of ras: the CAAX motif targets proteins to the ER and Golgi. *Cell.* 98:69–80.

Czech, M.P. 1995. Molecular actions of insulin on glucose transport. *Annu. Rev. Nutr.* 15:441–471.

Czech, M.P. 2000. PIP2 and PIP3: complex roles at the cell surface. *Cell.* 100:603–606.

Dupree, P., R.G. Parton, G. Raposo, and T.V. Kurzchalia. 1993. Caveolae and sorting in the trans-Golgi network of epithelial cells. *EMBO J.* 12:1597–1605.

Fujimoto, T., H. Hagiwara, T. Aoki, H. Kogo, and R. Nomura. 1998. Caveolae: from a morphological point of view. *J. Electron Microsc. (Tokyo).* 47:451–460.

Guilherme, A., and M.P. Czech. 1998. Stimulation of IRS-1-associated phosphatidylinositol 3-kinase and Akt/protein kinase B but not glucose transport by beta1-integrin signaling in rat adipocytes. *J. Biol. Chem.* 273:33119–33122.

Gustavsson, J., S. Parpal, M. Karlsson, C. Ramsing, H. Thorn, M. Borg, M. Lindroth, K.H. Peterson, K.E. Magnusson, and P. Stralfors. 1999. Localization of the insulin receptor in caveolae of adipocyte plasma membrane. *FASEB J.* 13:1961–1971.

Hailstones, D., L.S. Sleer, R.G. Parton, and K.K. Stanley. 1998. Regulation of caveolin and caveolae by cholesterol in MDCK cells. *J. Lipid Res.* 39:369–379.

Hancock, J.F., A.I. Magee, J.E. Childs, and C.J. Marshall. 1989. All ras proteins are polyisoprenylated but only some are palmitoylated. *Cell.* 57:1167–1177.

Hancock, J.F., H. Paterson, and C.J. Marshall. 1990. A polybasic domain or palmitoylation is required in addition to the CAAX motif to localize p21ras to the plasma membrane. *Cell.* 63:133–139.

Horton, R.M., S.N. Ho, J.K. Pullen, H.D. Hunt, Z. Cai, and L.R. Pease. 1993. Gene splicing by overlap extension. *Methods Enzymol.* 217:270–279.

Imagawa, M., T. Tsuchiya, and T. Nishihara. 1999. Identification of inducible genes at the early stage of adipocyte differentiation of 3T3-L1 cells. *Biochem. Biophys. Res. Commun.* 254:299–305.

Isakoff, S.J., C. Taha, E. Rose, J. Marcusohn, A. Klip, and E.Y. Skolnik. 1995. The inability of phosphatidylinositol 3-kinase activation to stimulate GLUT4 translocation indicates additional signaling pathways are required for insulin-stimulated glucose uptake. *Proc. Natl. Acad. Sci. USA.* 92:10247–10251.

Jiang, T., G. Sweeney, M.T. Rudolf, A. Klip, A. Traynor-Kaplan, and R.Y. Tsien. 1998. Membrane-permeant esters of phosphatidylinositol 3,4,5-trisphosphate. *J. Biol. Chem.* 273:11017–11024.

Kok, J.W., K. Hoekstra, S. Eskelinen, and D. Hoekstra. 1992. Recycling pathways of glucosylceramide in BHK cells: distinct involvement of early and late endosomes. *J. Cell Sci.* 103:1139–1152.

Krook, A., J.P. Whitehead, S.P. Dobson, M.R. Griffiths, M. Ouwens, C. Baker, A.C. Hayward, S.K. Sen, J.A. Maassen, K. Siddle, J.M. Tavare, and S. O'Rahilly. 1997. Two naturally occurring insulin receptor tyrosine kinase domain mutants provide evidence that phosphoinositide 3-kinase activation alone is not sufficient for the mediation of insulin's metabolic and mitogenic effects. *J. Biol. Chem.* 272:30208–30214.

Kurzchalia, T.V., and R.G. Parton. 1999. Membrane microdomains and caveolae. *Curr. Opin. Cell Biol.* 11:424–431.

Li, S., J. Couet, and M.P. Lisanti. 1996. Src tyrosine kinases, Galpha subunits, and H-Ras share a common membrane-anchored scaffolding protein, caveolin. Caveolin binding negatively regulates the auto-activation of Src tyrosine kinases. *J. Biol. Chem.* 271:29182–29190.

Lippincott-Schwartz, J., J.G. Donaldson, A. Schweizer, E.G. Berger, H.P. Hauri, L.C. Yuan, and R.D. Klausner. 1990. Microtubule-dependent retrograde transport of proteins into the ER in the presence of brefeldin A suggests an ER recycling pathway. *Cell.* 60:821–836.

Martin, S., J. Tellam, C. Livingstone, J.W. Slot, G.W. Gould, and D.E. James. 1996a. The glucose transporter (GLUT-4) and vesicle-associated membrane protein-2 (VAMP-2) are segregated from recycling endosomes in insulin-sensitive cells. *J. Cell Biol.* 134:625–635.

Martin, S.S., T. Haruta, A.J. Morris, A. Klippel, L.T. Williams, and J.M. Olefsky. 1996b. Activated phosphatidylinositol 3-kinase is sufficient to mediate actin rearrangement and GLUT4 translocation in 3T3-L1 adipocytes. *J. Biol. Chem.* 271:17605–17608.

Mastick, C.C., and A.R. Saltiel. 1997. Insulin-stimulated tyrosine phosphorylation of caveolin is specific for the differentiated adipocyte phenotype in 3T3-L1 cells. *J. Biol. Chem.* 272:20706–20714.

Mastick, C.C., M.J. Brady, and A.R. Saltiel. 1995. Insulin stimulates the tyrosine phosphorylation of caveolin. *J. Cell Biol.* 129:1523–1531.

Michaelson, D., J. Silletti, G. Murphy, P. D'Eustachio, M. Rush, and M.R. Philips. 2001. Differential localization of Rho GTPases in live cells. Regulation by hypervariable regions and RhoGDI binding. *J. Cell Biol.* 152:111–126.

Millar, C.A., A. Shewan, G.R. Hickson, D.E. James, and G.W. Gould. 1999. Differential regulation of secretory compartments containing the insulin-responsive glucose transporter 4 in 3T3-L1 adipocytes. *Mol. Biol. Cell.* 10:3675–3688.

Mineo, C., G.L. James, E.J. Smart, and R.G. Anderson. 1996. Localization of epidermal growth factor-stimulated Ras/Raf-1 interaction to caveolae membrane. *J. Biol. Chem.* 271:11930–11935.

Moodie, S.A., J. Alleman-Sposeto, and T.A. Gustafson. 1999. Identification of the APS protein as a novel insulin receptor substrate. *J. Biol. Chem.* 274:11186–11193.

Neudauer, C.L., G. Joberty, N. Tatsis, and I.G. Macara. 1998. Distinct cellular effects and interactions of the Rho-family GTPase TC10. *Curr. Biol.* 8:1151–1160.

Nobes, C.D., and A. Hall. 1995. Rho, rac, and cdc42 GTPases regulate the assembly of multimolecular focal complexes associated with actin stress fibers, lamellipodia, and filopodia. *Cell.* 81:53–62.

Nystrom, F.H., H. Chen, L.N. Cong, Y. Li, and M.J. Quon. 1999. Caveolin-1 interacts with the insulin receptor and can differentially modulate insulin signaling in transfected Cos-7 cells and rat adipose cells. *Mol. Endocrinol.* 13:2013–2024.

Okada, T., Y. Kawano, R. Sakakibara, O. Hazeki, and M. Ui. 1994. Essential role of phosphatidylinositol 3-kinase in insulin-induced glucose transport and antilipolysis in rat adipocytes. Studies with a selective inhibitor wortmannin. *J. Biol. Chem.* 269:3568–3573.

Okamoto, T., A. Schlegel, P.E. Scherer, and M.P. Lisanti. 1998. Caveolins, a family of scaffolding proteins for organizing "preassembled signalling complexes" at the plasma membrane. *J. Biol. Chem.* 273:5419–5422.

Parpal, S., M. Karlsson, H. Thorn, and P. Stralfors. 2001. Cholesterol depletion disrupts caveolae and insulin receptor signaling for metabolic control via insulin receptor substrate-1, but not for mitogen-activated protein kinase control. *J. Biol. Chem.* 276:9670–9678.

Pessin, J., D. Thurmond, J. Elmendorf, K. Coker, and S. Okada. 1999. Molecular basis of insulin-stimulated GLUT4 vesicle trafficking: Location! Location! Location! *J. Biol. Chem.* 274:2593–2596.

Pol, A., R. Luetterforst, M. Lindsay, S. Heino, E. Ikonen, and R.G. Parton. 2001. A caveolin dominant negative mutant associates with lipid bodies and induces intracellular cholesterol imbalance. *J. Cell Biol.* 152:1057–1070.

Prior, I.A., and J.F. Hancock. 2001. Compartmentalization of Ras proteins. *J. Cell Sci.* 114:1603–1608.

Rea, S., and D.E. James. 1997. Moving GLUT4: the biogenesis and trafficking of GLUT4 storage vesicles. *Diabetes.* 46:1667–1677.

Resh, M.D. 1999. Fatty acylation of proteins: new insights into membrane targeting of myristoylated and palmitoylated proteins. *Biochim. Biophys. Acta.* 1451:1–16.

Ribon, V., J.A. Printen, N.G. Hoffman, B.K. Kay, and A.R. Saltiel. 1998. A novel, multifuntional c-Cbl binding protein in insulin receptor signaling in 3T3-L1 adipocytes. *Mol. Cell. Biol.* 18:872–879.

Robinson, L.J., S. Pang, D.S. Harris, J. Heuser, and D.E. James. 1992. Translocation of the glucose transporter (GLUT4) to the cell surface in permeabilized 3T3-L1 adipocytes: effects of ATP and GTPγS and localization of GLUT4 to clathrin lattices. *J. Cell Biol.* 117:1181–1196.

Rothberg, K.G., J.E. Heuser, W.C. Donzell, Y.S. Ying, J.R. Glenney, and R.G. Anderson. 1992. Caveolin, a protein component of caveolae membrane coats. *Cell.* 68:673–682.

Roy, S., R. Luetterforst, A. Harding, A. Apolloni, M. Etheridge, E. Stang, B. Rolls, J.F. Hancock, and R. Parton. 1999. Dominant-negative caveolin inhibits H-Ras function by disrupting cholesterol-rich plasma membrane domains. *Nat. Cell Biol.* 1:98–105.

Seabra, M.C. 1998. Membrane association and targeting of prenylated Ras-like GTPases. *Cell Signal.* 10:167–172.

Severs, N.J. 1988. Caveolae: static inpocketings of the plasma membrane, dynamic vesicles or plain artifact. *J. Cell Sci.* 90:341–348.

Sharma, P.M., K. Egawa, Y. Huang, J.L. Martin, I. Huvar, G.R. Boss, and J.M. Olefsky. 1998. Inhibition of phosphatidylinositol 3-kinase activity by adenovirus-mediated gene transfer and its effect on insulin action. *J. Biol. Chem.* 273:18528–18537.

Simpson, F., J.P. Whitehead, and D.E. James. 2001. GLUT4--at the cross roads between membrane trafficking and signal transduction. *Traffic.* 2:2–11.

Smart, E.J., G.A. Graf, M.A. McNiven, W.C. Sessa, J.A. Engelman, P.E. Scherer, T. Okamoto, and M.P. Lisanti. 1999. Caveolins, liquid-ordered domains, and signal transduction. *Mol. Cell. Biol.* 19:7289–7304.

Song, K.S., S. Li, T. Okamoto, L.A. Quilliam, M. Sargiacomo, and M.P. Lisanti. 1996. Co-purification and direct interaction of Ras with caveolin, an integral membrane protein of caveolae microdomains. Detergent-free purification of caveolae microdomains. *J. Biol. Chem.* 271:9690–9697.

Sternberg, P.W., and S.L. Schmid. 1999. Caveolin, cholesterol and Ras signalling. *Nat. Cell Biol.* 1:E35–E37.

Summers, S.A., V.P. Yin, E.L. Whiteman, L.A. Garza, H. Cho, R.L. Tuttle, and M.J. Birnbaum. 1999. Signaling pathways mediating insulin-stimulated glucose transport. *Ann. NY Acad. Sci.* 892:169–186.

Vignal, E., M. De Toledo, F. Comunale, A. Ladopoulou, C. authier-Rouviere, A. Blangy, and P. Fort. 2000. Characterization of TCL, a New GTPase of the Rho Family related to TC10 and Cdc42. *J. Biol. Chem.* 275:36457–36464.

Voldstedlund, M., J. Tranum-Jensen, and J. Vinten. 1993. Quantitation of Na+/K(+)-ATPase and glucose transporter isoforms in rat adipocyte plasma membrane by immunogold labeling. *J. Membr. Biol.* 136:63–73.

Walsh, A.B., and D. Bar-Sagi. 2001. Differential activation of the rac pathway by ha-ras and k-ras. *J. Biol. Chem.* 276:15609–15615.

Watson, R.T., and J.E. Pessin. 2000. Functional cooperation of two independent targeting domains in syntaxin 6 is required for its efficient localization in the trans-Golgi network of 3T3L1 adipocytes. *J. Biol. Chem.* 275:1261–1268.

Weise, R.J., C.C. Mastick, D.F. Lazar, and A.R. Saltiel. 1995. Activation of mitogen-activated protein kinase and phosphatidylinositol 3′-kinase is not sufficient for the hormonal stimulation of glucose uptake, lipogenesis, or glycogen synthesis in 3T3-L1 adipocytes. *J. Biol. Chem.* 270:3442–3446.

Yamamoto, M., Y. Toya, C. Schwencke, M.P. Lisanti, M.G.J. Myers, and Y. Ishikawa. 1998. Caveolin is an activator of insulin receptor signaling. *J. Biol. Chem.* 273:26962–26968.